Am J Cancer Res 2023;13(12):6256-6269
www.ajcr.us /ISSN:2156-6976/ajcr0152571

Original Article

LncRNA SLC7A11-AS1 stabilizes CTCF by inhibiting its UBE3A-mediated ubiquitination to promote melanoma metastasis

Lingling Yu*, Jing Li*, Ming Xiao

*Department of Dermatology, Shanghai Eighth People's Hospital, Shanghai, China. *Equal contributors.*

Received August 2, 2023; Accepted November 28, 2023; Epub December 15, 2023; Published December 30, 2023

Abstract: Malignant melanoma (MM) is one of the most aggressive types of skin cancer. Long non-coding RNAs (lncRNAs) are important regulatory factors in the pathogenesis of various diseases. Here, we found that the lncRNA SLC7A11-AS1 was highly expressed in MM. Therefore, we investigated its regulatory role in the migration and invasion of MM cells and the associated mechanism. SLC7A11-AS1 and CTCF levels in MM cell lines were detected using RT-qPCR and western blotting, and their regulatory effects on the migratory and invasive abilities were determined using CCK-8, EdU, transwell, wound-healing assays and mouse model. RNA pull-down and RIP assays were performed to explore the association of SLC7A11-AS1 and CTCF and the correlation between CTCF and UBE3A. SLC7A11-AS1 and CTCF were highly expressed in MM cells. The knockdown of SLC7A11-AS1 decreased the expression of CTCF. Mechanistically, SLC7A11-AS1 inhibited the degradation of CTCF by inhibiting the ubiquitination by UBE3A. The knockdown of both SLC7A11-AS1 and CTCF inhibited the migration and invasion of MM cells and attenuated MM-to-lung metastasis in a mouse model. Taken together, SLC7A11-AS1 promoted the invasive and migratory abilities of MM cells by inhibiting the UBE3A-regulated ubiquitination of CTCF. Therefore, SLC7A11-AS1 may be a potential therapeutic target for MM.

Keywords: SLC7A11-AS1, CTCF, UBE3A, malignant melanoma, metastasis

Introduction

Malignant melanoma (MM) is a malignant tumor originating from melanocytes. It is the most aggressive form of skin cancer having stronger invasiveness, higher mortality, and poorer prognosis compared with other types of skin cancer [1]. Notably, the metastasis of MM cells is the main cause of mortality, and the 5-year survival rate is only 29.5% [2]. Despite the recent advances in diagnosis, immunotherapy, and molecularly targeted therapy, the prognosis of patients with MM remains poor. Moreover, patients may develop resistance to these treatments [3-6]. The global incidence of MM is annually increasing by approximately 3% [7], highlighting the need to identify effective biomarkers for early diagnosis and potential targets for developing new therapeutic strategies.

Long non-coding RNAs (lncRNAs) are non-protein-coding RNA molecules longer than 200 nucleotides [8]. They play a critical role in the treatment and diagnosis of malignant tumors by regulating gene expression at transcriptional, post-transcriptional, and epigenetic levels. Moreover, lncRNAs are involved in inducing and regulating cell cycle, growth, development, differentiation, proliferation, and apoptosis [9]. They can act as both promoters and suppressors in many pathophysiologic processes, including cancer cell growth, invasion, and metastasis. LncRNAs, such as BASP1-As1 and HOTAIR, are enriched in melanoma cells and can promote metastasis and cell proliferation and invasion while resisting apoptosis [10, 11]. Although the mechanism by which lncRNAs regulate tumor growth and metastasis has been extensively researched, few studies are available on MM-related lncRNAs. Screening of lncRNAs related to MM progression is essential to elucidating the underlying mechanism and identifying novel diagnostic, prognostic, and therapeutic strategies. LncRNA SLC7A11-AS1, a newly discovered lncRNA, is an antisense

Table 1. Oligonucleotide and primer sequences

Gene name	Name	Sequence (5'-3')
SLC7A11-AS1	Forward	AGCCTGGGTGATAAAGTG
	Reverse	TAAGCCCTCAATGGATAG
LncRNA Firre	Forward	CCTGTGACCTCGCTTCACTT
	Reverse	TTACACCCACTGTTGGCACC
GAPDH	Forward	CGCGAGAAGATGACCCAGAT
	Reverse	GGGCATACCCCTCGTAGATG
sh-lncRNA#1		CACCGCTACAGTCTAAATGCATACGCGAACGTATGCATTTAGACTGTAGC
sh-lncRNA#2		CACCGCACAGCACTTACTAGAAACTCGAAAGTTTCTAGTAAGTGCTGTGC
sh-NC		CACCCAGCTCCAACCAGCACCTGCGAACAG GTGCTGGTTGGAGCTG
sh-CTCF		CACCGCCCATAAACATAGGAGAACTCGAAA GTTCTCCTATGTTTATGGGC

transcript of the SLC7A11 gene. It is aberrantly expressed in multiple cancers, and its expression correlates with cancer cell metastasis. LncRNA SLC7A11-AS1 may play a tumor-promoting role in lung gastric, ovarian, and pancreatic cancers [12, 13]. However, whether SLC7A11-AS1 has a role in the development of MM remains unknown.

CCCTC binding factor (CTCF) is a chromatin-binding factor that binds to some specific sites of a DNA sequence [14]. It participates in transcriptional regulation by binding to chromatin insulators and blocks the interaction between promoters and nearby enhancers and silencers to regulate gene expression [15]. CTCF is involved in gene transcription, DNA repair, cell proliferation, and other physiologic functions [16, 17]. CTCF dysfunction may lead to tumors, such as gastric tumors [18-20]. Notably, CTCF may play contradictory roles in different tumors, and few reports are available on the mechanism by which CTCF affects the progression of MM.

Here, we first profiled the expression pattern of SLC7A11-AS in MM cell lines and human melanocytes. Subsequently, we investigated the role and mechanism by which SLC7A11-AS1 facilitates the migration and invasion (metastasis cascade) of MM cells. Our findings showed that SLC7A11-AS1 stabilizes CTCF by inhibiting the UBE3A-mediated ubiquitination to promote MM metastasis.

Materials and methods

Cell culture

Human MM cell lines, namely WM-115 (CAS: iCell-h225), A2058 (CAS: iCell-h310) and MV3 (CAS: iCell-h462), were obtained from iCell Bioscience Inc. Human MM cell line SK-MEL-5 (CAS: MZ-0685) was obtained from Ningbo Mingzhou Biotechnology Co., Ltd. HEMa-LP cell line (CAS: C0245C) was purchased from ThermoFisher Scientific. The cells were cultured in DMEM (Invitrogen) supplemented with 10% fetal bovine serum (ThermoFisher Scientific) and 1% streptomycin (100 mg/mL)/penicillin (100 U/mL; Invitrogen).

Quantitative PCR (RT-qPCR)

Total RNA was extracted using Trizol (Invitrogen). Cytoplasmic and nuclear RNAs were isolated using the cytoplasmic & nuclear RNA purification kit (Norgen Biotek). RNA was reverse transcribed using the PrimeScript RT Reagent Kit (Takara). RT-qPCR was performed using a TB Green Fast qPCR Mix Kit (Takara) or a Mir-X miRNA First-Strand Synthesis Kit (Takara). SLC7A11-AS1 expressions were normalized to that of GAPDH. The $2^{-\Delta\Delta Ct}$ method was used to quantify the RNA expression levels [21]. The primer sequences are listed in **Table 1**.

Transfection

Oligonucleotides encoding short hairpin RNA (shRNA) against SLC7A11-AS1 and CTCF (**Table 1**) were inserted into GV298 (GenePharma). The lentiviral vectors encoding sh-SLC7A11-AS1, sh-CTCF, and the respective controls (sh-NC) were synthesized by GenePharma. Lentiviral vectors were co-transfected with the packaging plasmids psPAX2 and pMD2G into HEK293T cells. Infectious lentiviruses were harvested at 48 h after transfection, followed with concentration by ultracentrifugation (2 h at 120,000 × g). Stable MM cell lines were obtained by selection with puromycin.

Transfection efficiency was determined using RT-qPCR.

Cell growth assay

Cell Counting Kit-8 (CCK-8; Beyotime) was used to determine cell growth. WM-115 and SK-MEL-5 cells (1 × 10^4 cells/well) transfected with sh-NC, sh-SLC7A11-AS1 or sh-CTCF were seeded into 96-well plates and incubated for 24, 48, and 72 h. The cells were then incubated in the CCK-8 solution for 2 h. Finally, OD values were measured at 450 nm using a microplate reader (Bio-Rad Laboratories).

5-Ethynyl-2'-deoxyuridine (EdU) assay

WM-115 and SK-MEL-5 cells (5 × 10^4 cells/well) were cultured in a six-well plate and transfected with sh-NC, sh-SLC7A11-AS1 or sh-CTCF. Cells were incubated in the Edu dye solution A (Invitrogen) for 2 h. The cells were then fixed in 4% paraformaldehyde for 15 min and gently washed twice with 3% BSA. The film was broken with 0.5% Triton X-100 for 20 min at room temperature, saturated with Click-it (provided in the EdU kit), and incubated in the dark for 30 min at room temperature. The cells were then washed twice with 3% BSA and stained with DAPI for 4 min. Finally, EdU-positive cell in each group was counted using Flow cytometry (BD).

Transwell assay

WM-115 and SK-MEL-5 cells (5 × 10^4) transfected with sh-NC, sh-SLC7A11-AS1 or sh-CTCF were resuspended in a serum-free medium (200 μL) and placed into the upper chamber of a Transwell plate having 8-μm pore size inserts and precoated with 50 μg of Matrigel (Millipore). The non-migrated cells were removed with a cotton swab after 48 h incubation. The migrated cells were fixed in 4% paraformaldehyde and stained with 0.5% crystal violet. Finally, the invading cells were counted and imaged under a microscope.

Wound-healing assay

WM-115 and SK-MEL-5 cells transfected with sh-NC, sh-SLC7A11-AS1 or sh-CTCF were cultured. A scratch wound was made in each cell monolayer using a sterile 10-μL pipette tip. The scratched cells were removed by washing with PBS, and serum-free DMEM was added to each well followed by incubation at 37°C for 48 h. Wound closure was imaged using an optical microscope (Leica) at 0 and 48 h, and migration distance was determined using ImageJ. Six to eight horizontal lines were randomly drawn to calculate the mean distance between cells.

Western blotting

Western blotting was performed to determine the protein expression levels [22]. Total protein lysates were lysed in RIPA lysis buffer (SIGMA; cat. no. R0278), and 20 μg of the cell lysate and 20 μl of conditioned media were separated on a 12% tris-glycine gel (Invitrogen, Carlsbad, CA), and the separated proteins were transferred to a PVDF membrane for immunoblotting (Millipore, Billerica, MA). The unoccupied sites were blocked using 5% skim milk dissolved in 1 × tris-buffered saline for 1 h at room temperature. The blocked membranes were incubated overnight with primary antibodies at 4°C, washed with TBST, and incubated with HRP-conjugated secondary antibodies at room temperature for 1 h. Immunoreactive bands were visualized using an ECL kit (ThermoFisher Scientific, 32106). The films were scanned using a ChemiDoc Touch imaging system (BIO-red), and the images were analyzed using ImageJ. The primary antibodies procured from Cell Signaling Technology were anti-GAPDH (1:2,000; cat. no. 5174), N-cadherin (1:1,000; cat. no. 13116), E-cadherin (1:1,000; cat. no. 14472), MMP2 (1:1,000; cat. no. 40994), and MMP9 (1:1,000; cat. no. 13667). UBE3A (1:1,000; cat. no. APREST81436) and CTCF (1:1,000; cat. no. AMAB90663) were procured from Sigma Aldrich, Inc. HRP-conjugated anti-rabbit IgG (1:1,000; cat. no. 7074) and anti-mouse IgG (1:1,000; cat. no. 7076) antibodies were procured from Cell Signaling Technology.

MM-to-lung metastasis model in nude mice

Five-week-old male BALB/c nude mice were purchased from Shanghai Jiaotong University (SCXK [Shanghai] 2018-0007). The protocols involving animals were approved by the Medicine Animal Care and Use Committee of Shanghai Eighth People's Hospital. The experiments were performed in strict compliance with institutional guidelines. WM-115 cells (2 × 10^5) transfected with sh-NC, sh-SLC7A11-AS1 or sh-CTCF lentivirus were suspended in 100 μL of PBS and injected into the tail vein of mice. The body weight of each mouse was recorded

every third day. No deaths occurred after implanting tumor cells. The mice were euthanized after 15 days, and the lungs were resected and fixed in 3.7% formaldehyde. The numbers of metastatic nodules in 1-mm-thick hematoxylin and eosin (H&E)-stained serial lung tissue sections were counted to evaluate tumor metastasis [23].

Bioinformatics analysis

RNAInter (http://rna-society.org/rnainter/) and PRIdictor websites (http://bclab.inha.ac.kr/pridictor/pridictor.html) were used to predict the putative binding sites between SLC7A11-AS1. Lysine modification sites were acquired from Protein Lysine Modification Database (PLMD, http://plmd.biocuckoo.org/). GEPIA (http://gepia.cancer-pku.cn/index.html) was used to determine the levels of SLC7A11-AS1 in human melanoma tissue.

RNA pull-down assay

Biotin-labeled sense and antisense SLC7A11-AS1, and biotin-CTCF were designed by Genechem and transfected into WM-115 and SK-MEL-5 cells for two days. Cell lysates obtained using Pierce IP Lysis Buffer (cat. no. 87788; ThermoFisher Scientific) were incubated with the labeled RNAs for 2 h. Subsequently, M-280 streptavidin-coated magnetic beads (Invitrogen) were added. The RNA/probe-coated bead mixtures were washed off and eluted using lysis and high-salt buffers. The precipitated components were analyzed using RT-qPCR.

RNA immunoprecipitation (RIP) assays

Approximately 2 × 10^7 WM-115 and SK-MEL-5 cells were lysed in RIP lysis buffer and incubated overnight with anti-*CTCF* (cat. no. PA5-41442; ThermoFisher Scientific), or normal anti-mouse IgG (cat. no. M4280, Sigma) antibodies at 4°C. Cell lysates were incubated with magnetic beads at 4°C for 1 h and then with proteinase K for 1 h at 55°C. RNA was subsequently extracted and purified, and the levels of GAPDH, SLC7A11-AS1 and lncRNA Firre were determined using RT-qPCR and normalized to the input RNA levels.

Statistical analyses

Data were analyzed using SPSS v.21 (IBM Corporation) and presented as means ± SD. Differences between the two groups were evaluated using the Student's *t*-test, whereas differences between multiple groups were examined using ANOVA followed by Tukey's test. Each experiment was performed in triplicate. *P*-values of < 0.05 or < 0.01 were considered statistically significant.

Results

SLC7A11-AS1 enhanced the invasion and migration of MM cells

SLC7A11-AS1 is one of the most frequently upregulated lncRNAs in cancer cells [24]. We found that SLC7A11-AS1 levels were markedly higher in MM cells compared with normal human epidermal melanocytes (all $P < 0.01$; **Figure 1A**). GEPIA (http://gepia.cancer-pku.cn/index.html) analysis also showed that the expression of SLC7A11-AS1 in the melanoma tissues was significantly higher than that in the normal tissues (**Figure 1B**). WM-115 and SK-MEL-5 cells were used for subsequent experiments because of the higher expression of SLC7A11-AS1 in these cells compared with other MM cells.

We first generated WM-115 and SK-MEL-5 cell lines stably expressing sh-SLC7A11-AS1 to explore the effect of lncRNA SLC7A11-AS1 on the invasive and migratory abilities of MM cells. Sh-lncRNA#1 or sh-lncRNA#2 lentiviral transfection reduced the expression of SLC7A11-AS1 by approximately 75% in WM-115 cells and 72% in SK-MEL-5 cells compared with the corresponding control (sh-NC, $P < 0.01$) shown in **Figure 1C**. CCK-8 assay was performed to investigate the effect of knocking down SLC7A11-AS1 on the growth of WM-115 and SK-MEL-5 cells. Compared with sh-NC, the sh-lncRNA#1- and sh-lncRNA#2-mediated knockdown of SLC7A11-AS1 significantly inhibited the viability of WM-115 and SK-MEL-5 cells at 24, 48, and 72 h (both $P < 0.01$; **Figure 1D**, **1E**). EdU-positive cell counts decreased after the knockdown of SLC7A11-AS1 in WM-115 and SK-MEL-5 cells in the SLC7A11-AS1 knockdown group compared with the sh-NC group (**Figure 1F-I**). Similarly, the results of the transwell assay showed that the invasive ability of WM-115 ($P < 0.01$; **Figure 1J**, **1K**) and SK-MEL-5 ($P < 0.01$; **Figure 1L**, **1M**) cells was reduced when SLC7A11-AS1 expression was inhibited. In addition, the results of wound-healing assay revealed a decrease in the migratory capacity

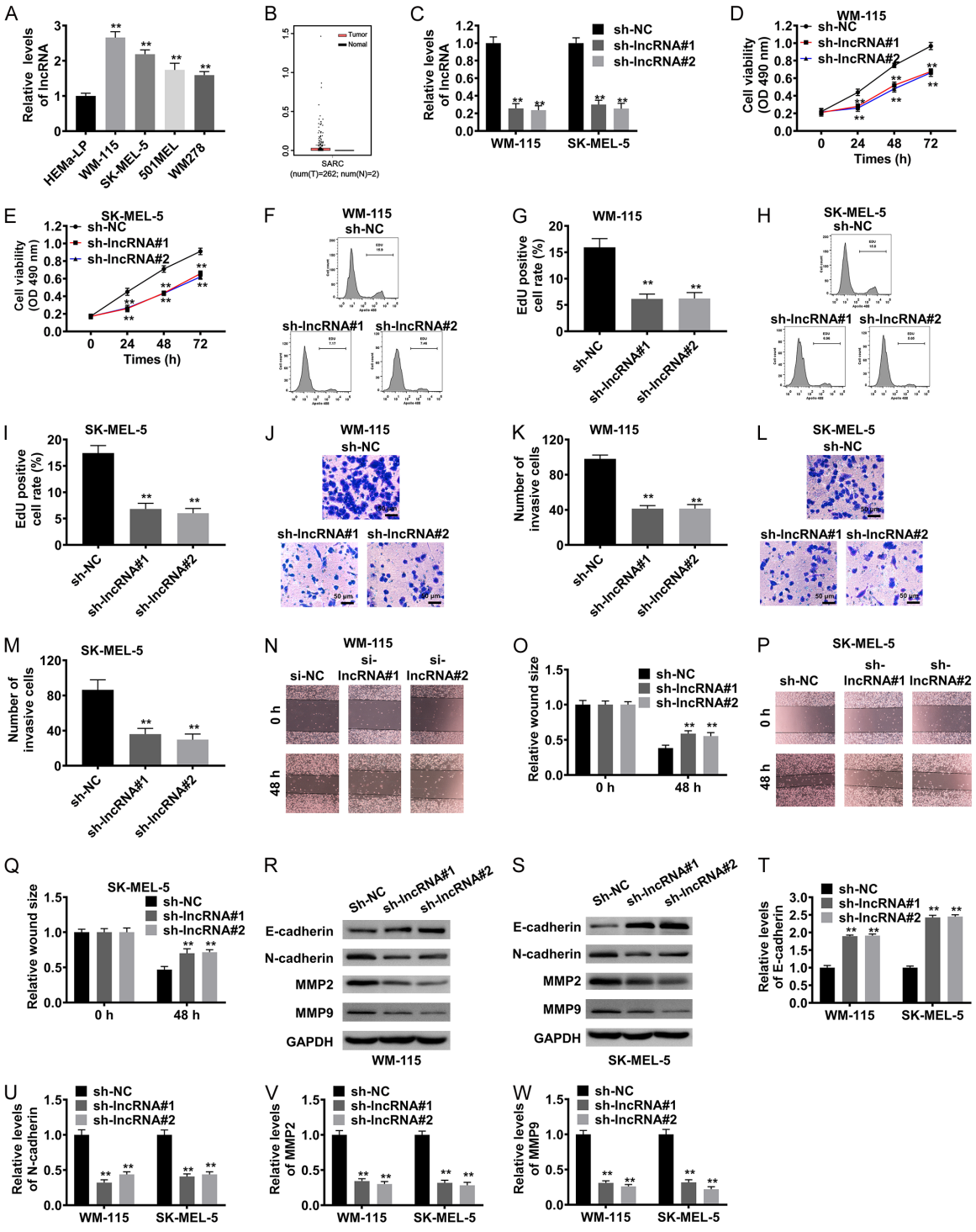

Figure 1. Knockdown of SLC7A11-AS1 inhibits the growth, proliferation, invasion, and migration of human melanoma cells. A. Expression of SLC7A11-AS1 in MM cell lines and normal human epidermal melanocytes (HEMa-LP) determined using RT-qPCR. B. SLC7A11-AS1 expression in human tissues determined using GEPIA. C. SLC7A11-AS1 expression determined using RT-qPCR after SLC7A11-AS1 knockdown. D, E. Viability of sh-SLC7A11-AS1-transfected WM-115 and SK-MEL-5 cells was detected using Cell Counting Kit-8 (CCK-8) assay. F-I. Proliferation of sh-SLC7A11-AS1-transfected WM-115 and SK-MEL-5 cells was detected using Edu staining assay. J-M. Invasive ability was examined using transwell assay (Scale bar: 50 μm). N-Q. Migratory ability of sh-SLC7A11-AS1-transfected WM-115 and SK-MEL-5 cells was determined using wound-healing assay (100 ×). R-W. Levels of E-cadherin, N-cadherin, MMP2, and MMP9 were determined using western blotting after SLC7A11-AS1 knockdown.

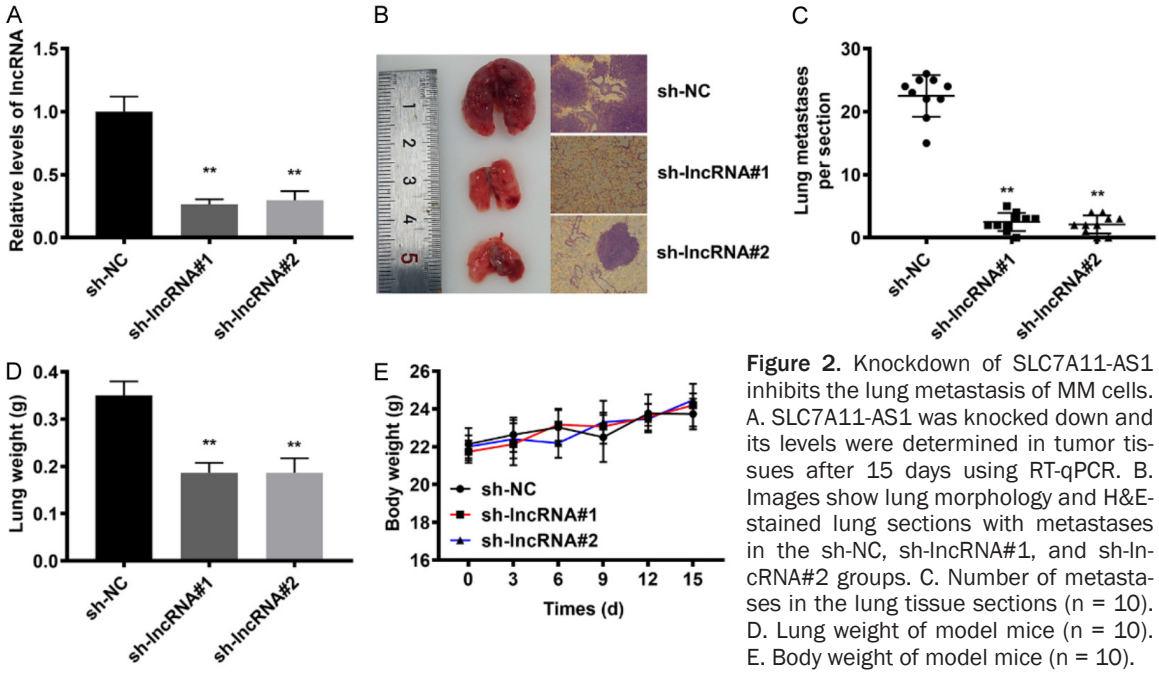

Figure 2. Knockdown of SLC7A11-AS1 inhibits the lung metastasis of MM cells. A. SLC7A11-AS1 was knocked down and its levels were determined in tumor tissues after 15 days using RT-qPCR. B. Images show lung morphology and H&E-stained lung sections with metastases in the sh-NC, sh-lncRNA#1, and sh-lncRNA#2 groups. C. Number of metastases in the lung tissue sections (n = 10). D. Lung weight of model mice (n = 10). E. Body weight of model mice (n = 10).

of both cell types after SLC7A11-AS1 knockdown (both $P < 0.01$; **Figure 1N-Q**). Moreover, SLC7A11-AS1 knockdown increased E-cadherin levels in WM-115 ($P < 0.01$; **Figure 1R**, **1T**) and SK-MEL-5 ($P < 0.01$; **Figure 1S**, **1T**) cells and decreased those expression of N-cadherin, MMP2, and MMP9 (all $P < 0.01$; **Figure 1R**, **1S**, **1U-W**). Overall, the silencing of SLC7A11-AS1 decreased the proliferative, invasive, and migratory potential of MM cells.

SLC7A11-AS1 depletion inhibited MM pulmonary metastasis in a mouse model

The lungs are the most common site of metastasis in patients with MM [23]. Therefore, WM-115 cells transfected with sh-SLC7A11-AS1 or sh-NC were injected into the tail vein of BALB/c nude mice to investigate whether SLC7A11-AS1 can inhibit the metastasis of MM to the lungs (**Figure 2A**). The number of tumor nodules within the lungs of the mice was determined in H&E-stained lung tissue sections 14 days after injecting the transfected cells (**Figure 2B**). Mice injected with sh-NC-transfected cells had large metastatic lesions, and the tumors in the lungs had clear boundaries. In contrast, the lungs of mice injected with sh-lncRNA#1 and sh-lncRNA#2-transfected cells displayed small and scattered metastatic lesions. Mice in the sh-NC group had 15-25 nodules in the lung tissues, whereas those in the sh-lncRNA#1 and sh-lncRNA#2 groups had 0-5 nodules ($P < 0.01$; **Figure 2C**). The body weight of the mice was evaluated every 3 days for 15 days, and the weights of the lungs were measured after resection. The weights of the lungs of mice from the sh-lncRNA#1 and sh-lncRNA#2 groups were lower than those of mice from the sh-NC group ($P < 0.01$; **Figure 2D**); However, no differences in body weight were observed among the three groups (**Figure 2E**). Overall, these results suggested that depleting SLC7A11-AS1 levels can inhibit the lung metastasis of MM.

SLC7A11-AS1 interacted with CTCF and maintained its expression in MM cells

Given that the function of SLC7A11-AS1 is associated with its subcellular localization [25-27], we first isolated cytoplasmic and nuclear RNA from MM cells to determine its localization. The RT-qPCR results showed that approximately 80% and 75% of SLC7A11-AS1 expression was localized to the cytoplasm of WM-115 and SK-MEL-5 cells, respectively. In contrast, only approximately 20% and 25% of expression was observed in the nucleus of WM-115 and SK-MEL-5 cells, respectively (both $P < 0.01$; **Figure 3A** and **3B**). Therefore, SLC7A11-AS1 was enriched in the cytoplasmic fraction of MM cells. The catRAPID, RNAInter, and miRDB database tools were used to predict the proteins and RNAs having putative binding sites for

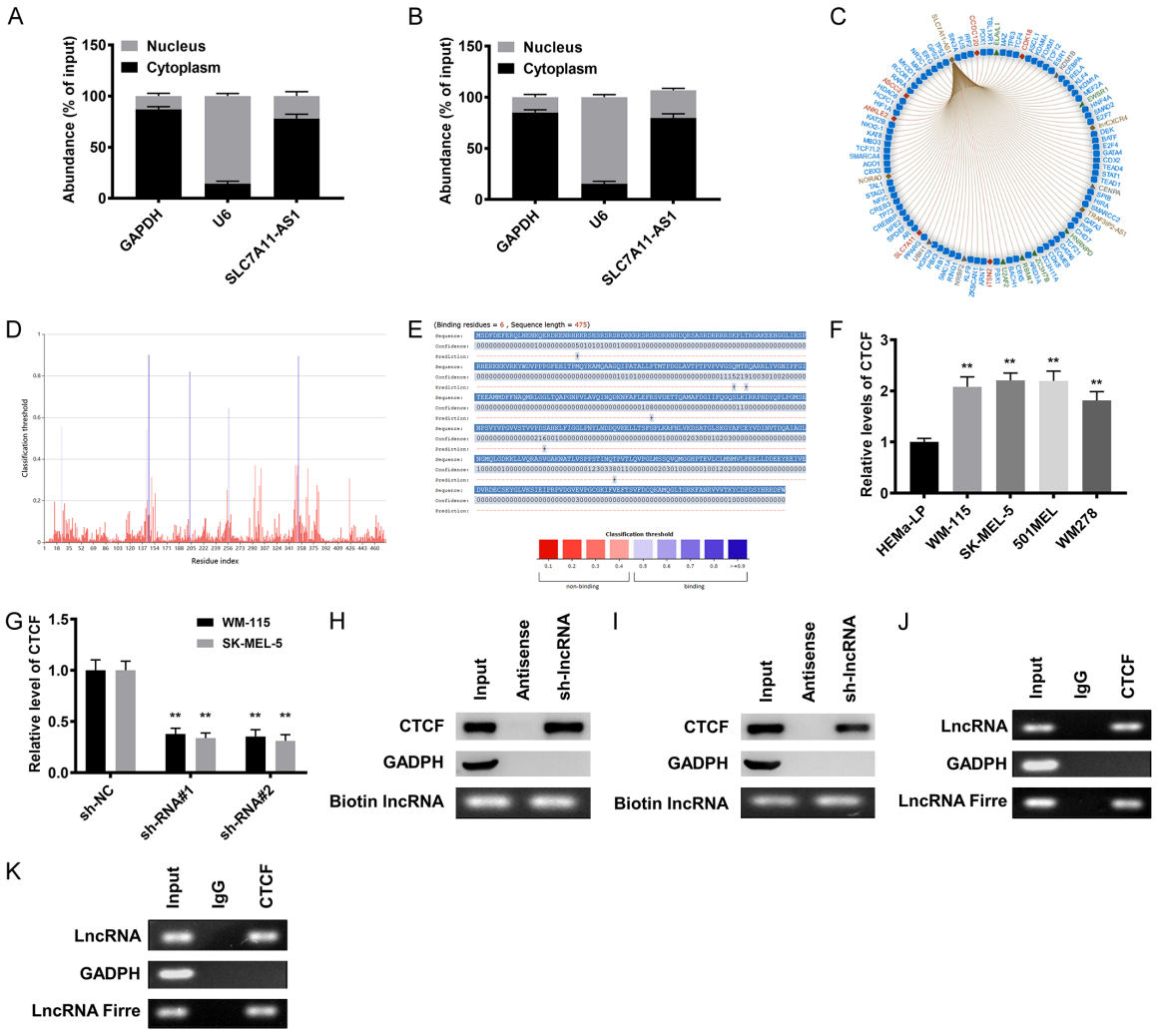

Figure 3. CTCF binds to SLC7A11-AS1 in melanoma cells. (A, B) RT-qPCR data shows that SLC7A11-AS1 was primarily localized in the cytoplasm of WM-115 and SK-MEL-5 cells. (C) Downstream targets of SLC7A11-AS1 predicted using bioinformatic analysis. The binding sites of CTCF in SLC7A11-AS1 (D) and the binding sites of SLC7A11-AS1 in CTCF (E). (F) High expression of CTCF in WM-115 and SK-MEL-5 cells. (G) CTCF expression in WM-115 and SK-MEL-5 cells after the knockdown of SLC7A11-AS1. (H, I) RNA pull-down assay results showed the interaction between SLC7A11-AS1 and CTCF in WM-115 and SK-MEL-5 cells. (J, K) RIP assay results showed the enrichment of SLC7A11-AS1 and CTCF in WM-115 cells and SK-MEL-5 cells.

SLC7A11-AS1 (**Figure 3C**; Tables S1 and S2). We focused on CTCF because it plays a key role in the invasion and migration of MM cells [28, 29]. The binding sites on CTCF and SLC7A11-AS1 were shown in **Figure 3D**, **3E**. Interestingly, CTCF was highly expressed in MM cells (**Figure 3F**). Moreover, SLC7A11-AS1 knockdown significantly decreased the CTCF protein levels (**Figure 3G**). We performed RNA pull-down assays to verify whether CTCF could directly bind to SLC7A11-AS1. Biotinylated sense SLC7A11-AS1-but not antisense SLC7A11-AS1-could directly pull down in WM-155 (**Figure 3H**) and SK-MEL-5 (**Figure 3I**) cells. Furthermore, RIP assays were performed to identify CTCF-interacting RNAs, and the results showed that the CTCF antibody precipitated high amounts of SLC7A11-AS1 and lncRNA fire in WM-115 and SK-MEL-5 cells compared with an anti-IgG control antibody (**Figure 3J**, **3K**). Overall, these results suggested that SLC7A11-AS1 may directly and specifically sponge CTCF.

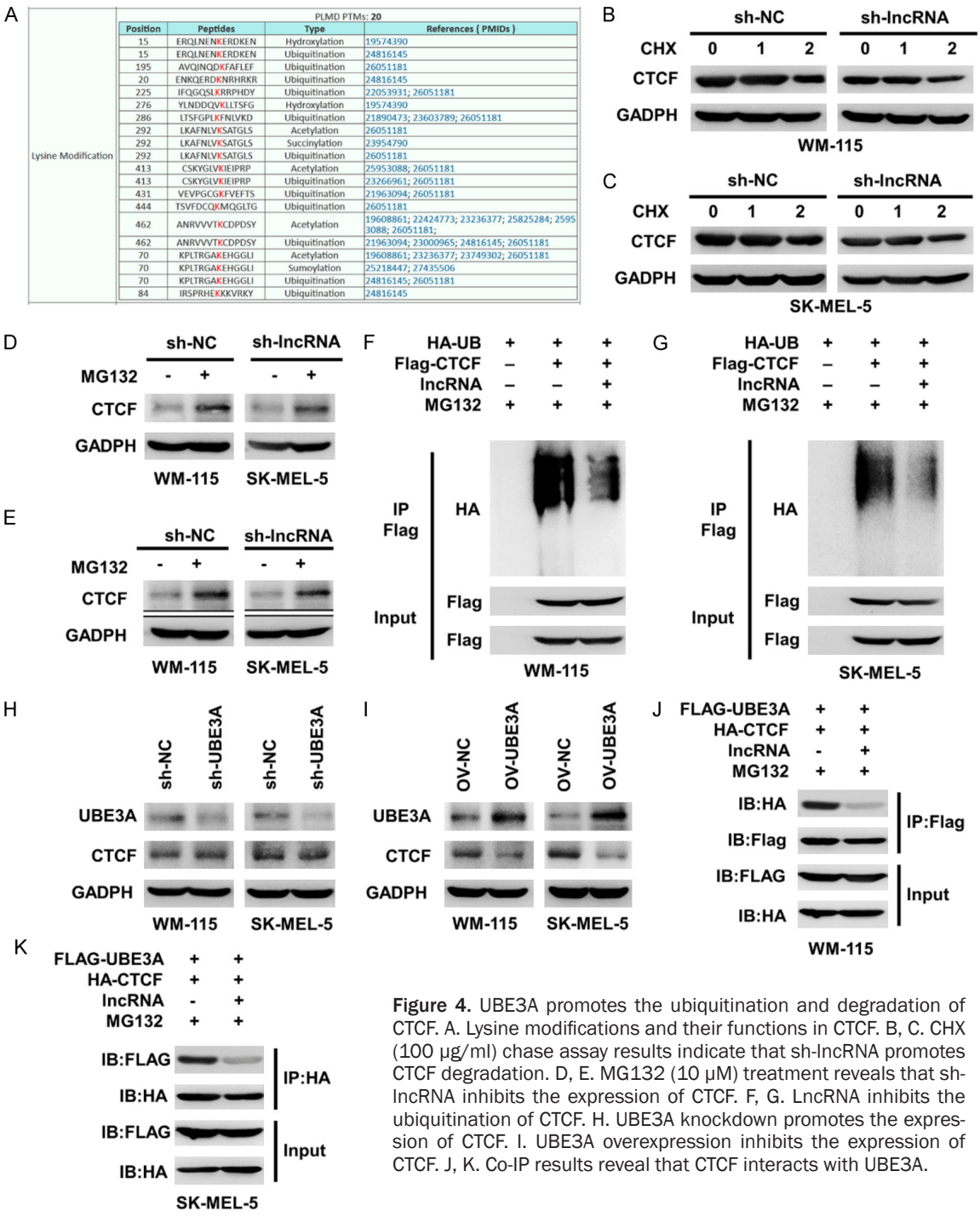

Figure 4. UBE3A promotes the ubiquitination and degradation of CTCF. A. Lysine modifications and their functions in CTCF. B, C. CHX (100 μg/ml) chase assay results indicate that sh-lncRNA promotes CTCF degradation. D, E. MG132 (10 μM) treatment reveals that sh-lncRNA inhibits the expression of CTCF. F, G. LncRNA inhibits the ubiquitination of CTCF. H. UBE3A knockdown promotes the expression of CTCF. I. UBE3A overexpression inhibits the expression of CTCF. J, K. Co-IP results reveal that CTCF interacts with UBE3A.

UBE3A promoted the ubiquitination and degradation of CTCF

Ubiquitin and E3 ligase play an important role in protein degradation. We screened the lysine modification sites and their functions in CTCF to determine whether CTCF is ubiquitinated by E3 ligase. Numerous ubiquitin modification sites were observed in CTCF (**Figure 4A**). The CHX chase assay showed that SLC7A11-AS1 knockdown showed a shorter CTCF half-life in WM-115 and SK-MEL-5 cells compared with sh-NC (**Figure 4B**, **4C**). The degradation of CTCF was inhibited by MG132, and the inhibitory effect of MG132 was ameliorated by SLC7A11-AS1 knockdown (**Figure 4D**, **4E**). Next, we deter-

mined the E3 ligase of CTCF and the mechanism by which SLC7A11-AS1 regulates CTCF degradation. Upregulation of SLC7A11-AS1 significantly decreased the ubiquitination of CTCF (**Figure 4F**, **4G**). We evaluated UBE3A as an E3 ligase responsible for the ubiquitination of CTCF. UBE3A knockdown increased the CTCF protein level (**Figure 4H**). However, the overexpression of UBE3A decreased the level of CTCF (**Figure 4I**). The co-immunoprecipitation results showed that SLC7A11-AS1 overexpression weakened the interaction between UBE3A and CTCF (**Figure 4J**, **4K**). Taken together, UBE3A promoted the ubiquitination and degradation of CTCF, which were regulated by SLC7A11-AS1.

Downregulation of CTCF inhibited the invasive and migratory abilities of MM cells

We measured the levels of CTCF in WM-115 and SK-MEL-5 cells and found that protein levels of CTCF were significantly lower in the sh-CTCF groups compared with those in the sh-NC groups (all $P < 0.01$; **Figure 5A**, **5B**). Sh-NC and sh-CTCF were then transfected into WM-115 and SK-MEL-5 cells to determine whether dysregulated CTCF expression affects the invasive and migratory capacity of MM lines. The CCK-8 assay results confirmed that sh-CTCF transfection decreased the viability of WM-115 cells at 24, 48, and 72 h compared with sh-NC transfection (**Figure 5C**). In addition, a similar effect was observed in SK-MEL-5 cells at the three time points (all $P < 0.01$; **Figure 5D**). EdU-positive cell counts significantly decreased after sh-CTCF transfection in WM-115 and SK-MEL-5 cells compared with those after sh-NC transfection (all $P < 0.01$; **Figure 5E-H**). Sh-CTCF suppressed the invasive ability of WM-115 cells by approximately 50% ($P < 0.01$; **Figure 5I**, **5J**) and that of SK-MEL-5 cells by approximately 40% ($P < 0.01$; **Figure 5K**, **5L**). A corresponding inhibitory effect on cell migration was observed after sh-CTCF transfection in both WM-115 ($P < 0.01$; **Figure 5M**, **5N**) and SK-MEL-5 ($P < 0.01$; **Figure 5O**, **5P**) cells. Moreover, sh-CTCF upregulated the levels of E-cadherin in both WM-115 and SK-MEL-5 cells (both $P < 0.01$; **Figure 5Q**, **5S**) and downregulated those of N-cadherin, MMP2, and MMP9 ($P < 0.01$ for both cell lines; **Figure 5Q**, **5R**, **5T-V**), indicating that the inhibition of CTCF rescued the MM cell invasion and migration.

Downregulation of CTCF inhibited pulmonary metastasis of MM in a mouse model

The effect of sh-CTCF on the metastatic ability of MM cells was assessed in a lung metastasis mouse model generated by injecting sh-CTCF-transfected (or sh-NC-transfected) WM-115 cells into the tail vein of mice (**Figure 6A**). **Figure 6B** shows the representative histopathologic images. Mice injected with sh-NC-transfected MM cells showed large metastatic lesions and their lung tumors had clear boundaries. In contrast, mice injected with sh-CTCF-transfected cells showed relatively small and scattered tumor masses in the lungs. Additionally, the average number of lung metastatic nodules was noticeably lower in mice from the sh-CTCF group compared with those from the sh-NC group. Mice in the sh-NC group had 18-27 nodules on the lung surface, whereas those in the sh-CTCF group had 0-5 nodules ($P < 0.01$; **Figure 6C**). The lung weight of mice in the sh-CTCF group was less than that of mice in the sh-NC group (**Figure 6D**). However, body weight was not significantly different between the two groups (**Figure 6E**). Overall, the downregulation of CTCF inhibited lung metastasis of MM in mice.

Discussion

LncRNAs regulate the progression of MM [30-32]. SLC7A11-AS1 is a sensitive and specific biomarker for various types of cancers, including pancreatic [25, 33] and lung cancers [24]. However, the role of SLC7A11-AS1 in the pathogenesis of MM remains unknown. Here, we found that SLC7A11-AS1 accelerated MM cell migration and invasion and promoted lung metastasis in a mouse model. Furthermore, we showed for the first time that SLC7A11-AS1 maintained CTCF stability by blocking UBE3A-mediated ubiquitination.

LncRNAs are involved in numerous biological processes. They may act as the activators of distinct transcriptional programs or as scaffolds for the ribonucleoprotein complexes. Additionally, lncRNAs can regulate the expression of genes at multiple levels. Therefore, investigating the functions of lncRNAs and the associated mechanisms will facilitate the understanding of the molecular mechanisms underlying tumorigenic processes. SLC7A11-

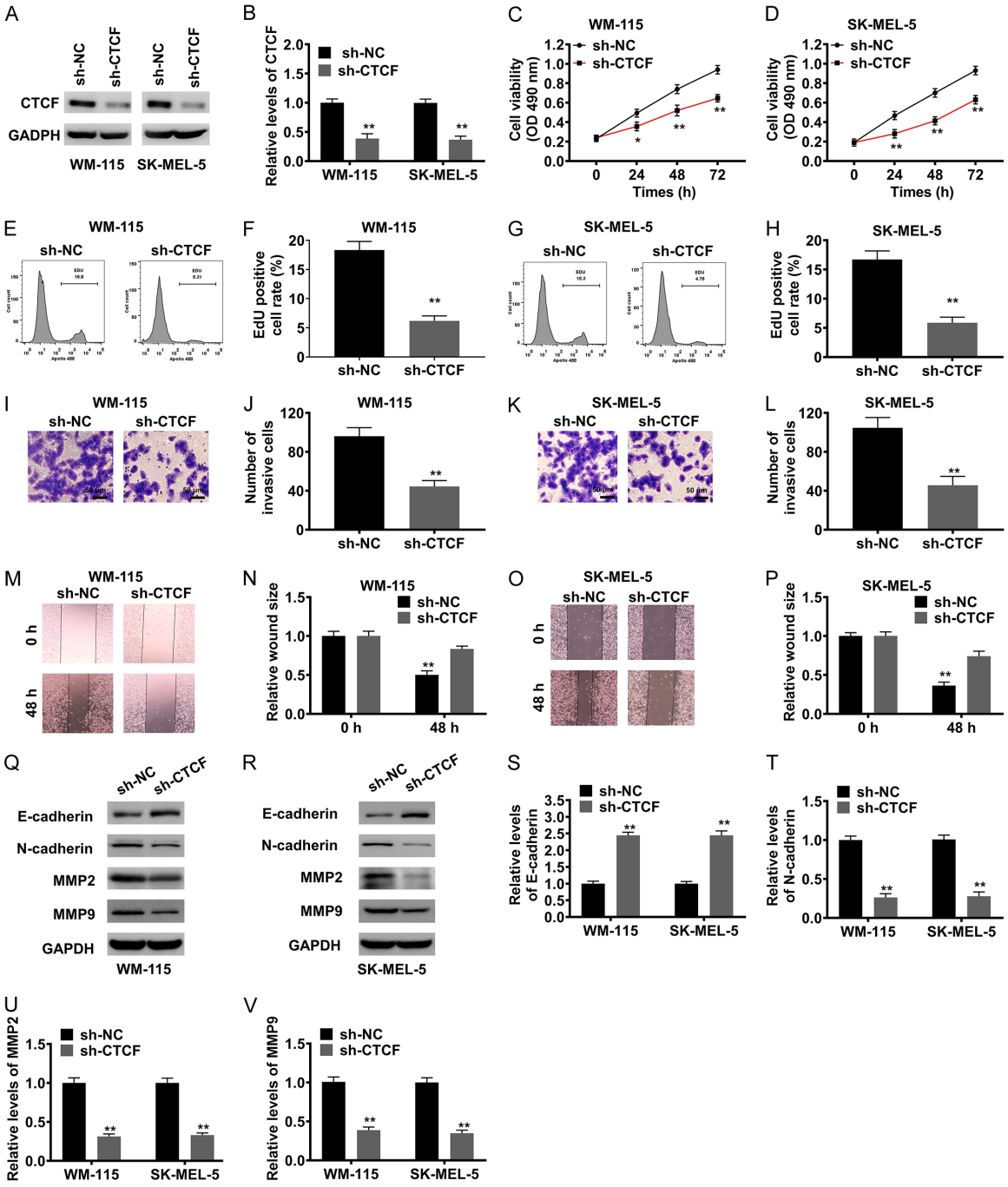

Figure 5. Downregulation of CTCF inhibits the invasive and migratory abilities of MM cell lines. A, B. CTCF protein level in WM-115 and SK-MEL-5 cells transfected with sh-CTCF determined using western blotting. C, D. Viability of WM-115 and SK-MEL-5 cells transfected with sh-CTCF determined using CCK-8 assay. E-H. Proliferation of sh-CTCF-transfected WM-115 and SK-MEL-5 cells determined Edu staining assay. I-L. Invasive ability of sh-CTCF transfected WM-115 and SK-MEL-5 cells determined using transwell assay (Scale bar: 50 μm). M-P. Migratory ability of sh-CTCF-transfected WM-115 and SK-MEL-5 cells detected using wound-healing assay (100 ×). Q-V. Levels of E-cadherin, N-cadherin, MMP2, and MMP9 in cells transfected with sh-CTCF detected using western blotting.

AS1 plays an oncogenic role in gastric and breast cancers [13, 34]. Yang *et al.* [33] reported that SLC7A11-AS1 expression was increased in pancreatic ductal adenocarcinoma (PDAC) tissues and gemcitabine-resistant cell lines. Additionally, SLC7A11-AS1 inhibition attenuat-

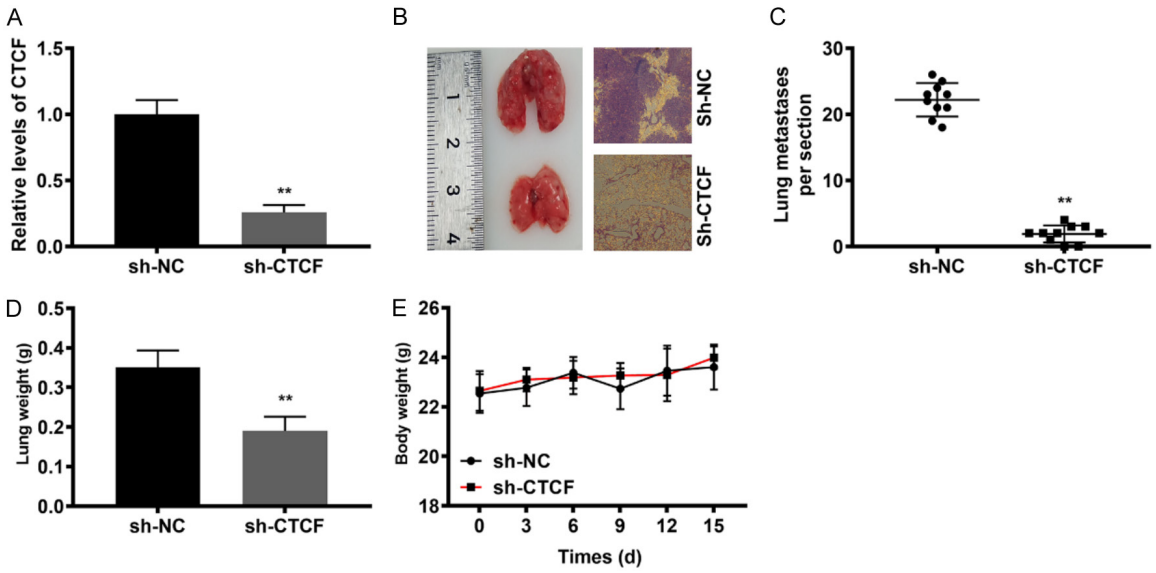

Figure 6. Inhibition of CTCF suppresses the lung metastasis of MM cells. A. CTCF was knocked down, and its levels in tumor tissues were determined after 15 days using western blotting. B. Images show the lung morphology and H&E-stained lung sections with metastases in the sh-NC and sh-CTCF groups. C. Numbers of metastases in the lung tissue sections (n = 10). D. Lung weight of model mice (n = 10). E. Body weight of model mice (n = 10).

ed PDAC stemness and increased the sensitivity of PDAC cells to gemcitabine. Liang *et al.* [26] found that SLC7A11-AS1 was closely correlated with the metastasis of hepatocellular carcinoma. However, whether SLC7A11-AS1 is aberrantly expressed in MM or plays a role in the pathogenesis of this malignancy remains unknown. We found that SLC7A11-AS1 was significantly upregulated in MM cell lines compared with normal human melanocytes, indicating the crucial role of SLC7A11-AS1 as an oncogene in MM. Liu *et al.* also reported that SLC7A11-AS1 levels increase in lung cancer, and it is involved as an oncogene in tumorigenesis [24]. In this study, we verified whether this lncRNA also exerts oncogenic functions in MM as in other tumors, such as PDAC [33] and lung cancer [24]. Therefore, we depleted SLC7A11-AS1 expression and evaluated the effect on the invasive and migratory potential of MM cells. The knockdown of SLC7A11-AS1 inhibited the invasion and migration of MM cells and inhibited lung metastasis in a mouse model. Taken together, SLC7A11-AS1 may function as an oncogene in MM.

The molecular mechanism underlying lncRNA activity depends on its subcellular localization. LncRNAs located in the cytoplasm, which can regulate protein expression by modulating protein ubiquitination [33] or through *cis*-regulatory mechanisms [34]. Here, we found that SLC7A11-AS1 was primarily localized to the cytoplasm in MM cells; therefore, we explored its function as a potential scaffold. In this study, we conducted a bioinformatic analysis and found that SLC7A11-AS1 contains a conserved target site for CTCF binding. The dysregulation of CTCF can exert both tumor-promoting and tumor-suppressing effects in various types of cancer. For example, high CTCF expression levels promoted the growth of breast cancer [35], osteosarcoma [36], and colorectal cancers [37], whereas CTCF downregulation inhibited cell proliferation and invasion and facilitated cell apoptosis [38]. These observations suggested that CTCF may be the downstream target of SLC7A11-AS1 in MM cells. Our results showed that SLC7A11-AS1 forms a complex with CTCF. SLC7A11-AS1 and CTCF were highly enriched in MM cell lines, providing further evidence that SLC7A11-AS1 regulation of MM metastasis is associated with CTCF. Interestingly, we identified that CTCF interacts with the UBE3A, an E3 ligase, by reviewing previous research. Additionally, we found that SLC7A11-AS1 antibody precipitated both CTCF and UBE3A, and *UBE3A* was strongly associated with the biotin-labeled CTCF probe in RNA pull-down assays. Furthermore, sh-UBE3A signifi-

cantly increased the CTCF protein levels. Altogether, SLC7A11-AS1 could regulate CTCF by directly inhibiting the binding of CTCF with UBE3A. We then explored whether the regulatory role of SLC7A11-AS1 in MM metastasis is exerted by upregulating CTCF. Sh-CTCF transfection rescued the growth, migration, and invasion of MM cells and further confirmed its inhibitory effect on mouse lung metastasis. These findings suggested that SLC7A11-AS1 promotes the invasion and migration of MM cells by inhibiting the UBE3A-mediated ubiquitination of CTCF.

However, our study has some limitations. First, we did not investigate the mechanisms and pathways through which *CTCF* enhances the malignant characteristics of tumor cells. In addition, we did not explore the effects of combining CTCF and SLC7A11-AS1 knockdown as a rescue experiment. Moreover, we did not determine whether SLC7A11-AS1 targets miRNAs while regulating MM metastasis or CTCF interacts with other proteins.

Conclusion

We found that SLC7A11-AS1 expression is upregulated in MM cell lines. SLC7A11-AS1 enhances the proliferative, invasive, and migratory abilities of MM cells *by* inhibiting UBE3A-mediated ubiquitination of CTCF. Our findings provide novel insights into the prevention and treatment of MM.

Disclosure of conflict of interest

None.

Address correspondence to: Ming Xiao, Department of Dermatology, Shanghai Eighth People's Hospital, No. 8 Caobao Road, Shanghai 200235, China. E-mail: 15618251797@163.com

References

[1] Miller KD, Nogueira L, Mariotto AB, Rowland JH, Yabroff KR, Alfano CM, Jemal A, Kramer JL and Siegel RL. Cancer treatment and survivorship statistics, 2019. CA Cancer J Clin 2019; 69: 363-385.

[2] Saginala K, Barsouk A, Aluru JS, Rawla P and Barsouk A. Epidemiology of melanoma. Med Sci (Basel) 2021; 9: 63.

[3] Yue J, Vendramin R, Liu F, Lopez O, Valencia MG, Gomes Dos Santos H, Gaidosh G, Beckedorff F, Blumenthal E, Speroni L, Nimer SD, Marine JC and Shiekhattar R. Targeted chemotherapy overcomes drug resistance in melanoma. Genes Dev 2020; 34: 637-649.

[4] Huang R and Rofstad EK. Integrins as therapeutic targets in the organ-specific metastasis of human malignant melanoma. J Exp Clin Cancer Res 2018; 37: 92.

[5] Liang L, Wen L, Weng Y, Song J, Li H, Zhang Y, He X, Zhao W, Zhan M and Li Y. Homologous-targeted and tumor microenvironment-activated hydroxyl radical nanogenerator for enhanced chemoimmunotherapy of non-small cell lung cancer. Chemical Engineering Journal 2021; 425: 131451.

[6] Li H, Zhang Y, Liang L, Song J, Wei Z, Yang S, Ma Y, Chen WR, Lu C and Wen L. Doxorubicin-loaded metal-organic framework nanoparticles as acid-activatable hydroxyl radical nanogenerators for enhanced chemo/chemodynamic synergistic therapy. Materials (Basel) 2022; 15: 1096.

[7] Sung H, Ferlay J, Siegel RL, Laversanne M, Soerjomataram I, Jemal A and Bray F. Global cancer statistics 2020: GLOBOCAN estimates of incidence and mortality worldwide for 36 cancers in 185 countries. CA Cancer J Clin 2021; 71: 209-249.

[8] Joshi M and Rajender S. Long non-coding RNAs (lncRNAs) in spermatogenesis and male infertility. Reprod Biol Endocrinol 2020; 18: 103.

[9] Xia H, Huang Z, Liu S, Zhao X, He R, Wang Z, Shi W, Chen W, Li Z, Yu L, Huang P, Kang P, Su Z, Xu Y, Yam JWP and Cui Y. LncRNA DiGeorge syndrome critical region gene 5: a crucial regulator in malignant tumors. Biomed Pharmacother 2021; 141: 111889.

[10] Wang J, Chen J, Jing G and Dong D. LncRNA HOTAIR promotes proliferation of malignant melanoma cells through NF-κB pathway. Iran J Public Health 2020; 49: 1931-1939.

[11] Li Y, Gao Y, Niu X, Tang M, Li J, Song B and Guan X. LncRNA BASP1-AS1 interacts with YBX1 to regulate notch transcription and drives the malignancy of melanoma. Cancer Sci 2021; 112: 4526-4542.

[12] Luo Y, Xiang W, Liu Z, Yao L, Tang L, Tan W, Ye P, Deng J and Xiao J. Functional role of the SLC7A11-AS1/xCT axis in the development of gastric cancer cisplatin-resistance by a GSH-dependent mechanism. Free Radic Biol Med 2022; 184: 53-65.

[13] Synnott NC, Madden SF, Bykov VJN, Crown J, Wiman KG and Duffy MJ. The mutant p53-targeting compound APR-246 induces ROS-modulating genes in breast cancer cells. Transl Oncol 2018; 11: 1343-1349.

[14] Fang C, Wang Z, Han C, Safgren SL, Helmin KA, Adelman ER, Serafin V, Basso G, Eagen KP,

Gaspar-Maia A, Figueroa ME, Singer BD, Ratan A, Ntziachristos P and Zang C. Cancer-specific CTCF binding facilitates oncogenic transcriptional dysregulation. Genome Biol 2020; 21: 247.

[15] Xiao T, Wongtrakoongate P, Trainor C and Felsenfeld G. CTCF recruits centromeric protein CENP-E to the pericentromeric/centromeric regions of chromosomes through unusual CTCF-binding sites. Cell Rep 2015; 12: 1704-14.

[16] Alpsoy A, Sood S and Dykhuizen EC. At the crossroad of gene regulation and genome organization: potential roles for ATP-dependent chromatin remodelers in the regulation of CTCF-mediated 3D architecture. Biology (Basel) 2021; 10: 272.

[17] Dehingia B, Milewska M, Janowski M and Pękowska A. CTCF shapes chromatin structure and gene expression in health and disease. EMBO Rep 2022; 23: e55146.

[18] Debaugny RE and Skok JA. CTCF and CTCFL in cancer. Curr Opin Genet Dev 2020; 61: 44-52.

[19] Sun L, Huang C, Zhu M, Guo S, Gao Q, Wang Q, Chen B, Li R, Zhao Y, Wang M, Chen Z, Shen B and Zhu W. Gastric cancer mesenchymal stem cells regulate PD-L1-CTCF enhancing cancer stem cell-like properties and tumorigenesis. Theranostics 2020; 10: 11950-11962.

[20] Segueni J and Noordermeer D. CTCF: a misguided jack-of-all-trades in cancer cells. Comput Struct Biotechnol J 2022; 20: 2685-2698.

[21] Li X, Deng S, Pang X, Song Y, Luo S, Jin L and Pan Y. LncRNA NEAT1 silenced miR-133b promotes migration and invasion of breast cancer cells. Int J Mol Sci 2019; 20: 3616.

[22] Zhang K, Wang A, Zhong K, Qi S, Wei C, Shu X, Tu WY, Xu W, Xia C, Xiao Y, Chen A, Bai L, Zhang J, Luo B, Wang W and Shen C. UBQLN2-HSP70 axis reduces poly-Gly-Ala aggregates and alleviates behavioral defects in the C9ORF72 animal model. Neuron 2021; 109: 1949-1962, e6.

[23] Wang X, Wang B, Zhan W, Kang L, Zhang S, Chen C, Hou D, You R and Huang H. Melatonin inhibits lung metastasis of gastric cancer in vivo. Biomed Pharmacother 2019; 117: 109018.

[24] Liu Y, Fan X, Zhao Z and Shan X. LncRNA SLC7A11-AS1 contributes to lung cancer progression through facilitating TRAIP expression by inhibiting miR-4775. Onco Targets Ther 2020; 13: 6295-6302.

[25] Xie W, Chu M, Song G, Zuo Z, Han Z, Chen C, Li Y and Wang ZW. Emerging roles of long noncoding RNAs in chemoresistance of pancreatic cancer. Semin Cancer Biol 2022; 83: 303-318.

[26] Liang J, Liao J, Liu T, Wang Y, Wen J, Cai N, Huang Z, Xu W, Li G, Ding Z and Zhang B. Comprehensive analysis of TGF-β-induced mRNAs and ncRNAs in hepatocellular carcinoma. Aging (Albany NY) 2020; 12: 19399-19420.

[27] Wang LX, Wan C, Dong ZB, Wang BH, Liu HY and Li Y. Integrative analysis of long noncoding RNA (lncRNA), microRNA (miRNA) and mRNA expression and construction of a competing endogenous RNA (ceRNA) network in metastatic melanoma. Med Sci Monit 2019; 25: 2896-2907.

[28] Yuan X, Pan J, Wen L, Gong B, Li J, Gao H, Tan W, Liang S, Zhang H and Wang X. MiR-590-3p regulates proliferation, migration and collagen synthesis of cardiac fibroblast by targeting ZEB1. J Cell Mol Med 2020; 24: 227-237.

[29] Zheng ZQ, Li ZX, Zhou GQ, Lin L, Zhang LL, Lv JW, Huang XD, Liu RQ, Chen F, He XJ, Kou J, Zhang J, Wen X, Li YQ, Ma J, Liu N and Sun Y. Long noncoding RNA FAM225A promotes nasopharyngeal carcinoma tumorigenesis and metastasis by acting as ceRNA to sponge miR-590-3p/miR-1275 and upregulate ITGB3. Cancer Res 2019; 79: 4612-4626.

[30] Chen X, Gao J, Yu Y, Zhao Z and Pan Y. LncRNA FOXD3-AS1 promotes proliferation, invasion and migration of cutaneous malignant melanoma via regulating miR-325/MAP3K2. Biomed Pharmacother 2019; 120: 109438.

[31] Xia Y, Zhou Y, Han H, Li P, Wei W and Lin N. lncRNA NEAT1 facilitates melanoma cell proliferation, migration, and invasion via regulating miR-495-3p and E2F3. J Cell Physiol 2019; 234: 19592-19601.

[32] Zhang S, Wan H and Zhang X. LncRNA LHFPL3-AS1 contributes to tumorigenesis of melanoma stem cells via the miR-181a-5p/BCL2 pathway. Cell Death Dis 2020; 11: 950.

[33] Yang Q, Li K, Huang X, Zhao C, Mei Y, Li X, Jiao L and Yang H. lncRNA SLC7A11-AS1 promotes chemoresistance by blocking SCF(β-TRCP)-mediated degradation of NRF2 in pancreatic cancer. Mol Ther Nucleic Acids 2020; 19: 974-985.

[34] Luo Y, Wang C, Yong P, Ye P, Liu Z, Fu Z, Lu F, Xiang W, Tan W and Xiao J. Decreased expression of the long non-coding RNA SLC7A11-AS1 predicts poor prognosis and promotes tumor growth in gastric cancer. Oncotarget 2017; 8: 112530-112549.

[35] Wong KM, Song J and Wong YH. CTCF and EGR1 suppress breast cancer cell migration through transcriptional control of Nm23-H1. Sci Rep 2021; 11: 491.

[36] Zhan H, Xiao J, Wang P, Mo F, Li K, Guo F, Yu X, Liu X, Zhang B, Dai M and Liu H. Exosomal CTCF confers cisplatin resistance in osteosarcoma by promoting autophagy via the IGF2-

AS/miR-579-3p/MSH6 axis. J Oncol 2022; 2022: 9390611.

[37] Lai Q, Li Q, He C, Fang Y, Lin S, Cai J, Ding J, Zhong Q, Zhang Y, Wu C, Wang X, He J, Liu Y, Yan Q, Li A and Liu S. CTCF promotes colorectal cancer cell proliferation and chemotherapy resistance to 5-FU via the P53-Hedgehog axis. Aging (Albany NY) 2020; 12: 16270-16293.

[38] Shan Z, Li Y, Yu S, Wu J, Zhang C, Ma Y, Zhuang G, Wang J, Gao Z and Liu D. CTCF regulates the FoxO signaling pathway to affect the progression of prostate cancer. J Cell Mol Med 2019; 23: 3130-3139.